

TopoCurate: Modeling Interaction Topology for Tool-Use Agent Training

Jinluan Yang^{1*} Yuxin Liu^{2*} Zhengyu Chen^{2*} Chengcheng Han^{2*} Yueqing Sun² Qi Gu² Hui Su²
Xunliang Cai² Fei Wu¹ Kun Kuang¹

Abstract

Training tool-use agents typically relies on outcome-based filtering: Supervised Fine-Tuning (SFT) on successful trajectories and Reinforcement Learning (RL) on pass-rate-selected tasks. However, this paradigm ignores interaction dynamics—successful trajectories may lack error recovery or exhibit redundancy, while pass rates fail to distinguish structurally informative tasks from trivial ones. We propose **TopoCurate**, an interaction-aware framework that projects multi-trial rollouts from the same task into a unified semantic quotient topology. By merging equivalent action-observation states, this projection transforms scattered linear trajectories into a structured manifold that explicitly captures how tool invocations and environmental responses drive the divergence between effective strategies and failure modes. Leveraging this representation, we introduce a dual-selection mechanism: for SFT, we prioritize trajectories demonstrating reflective recovery, semantic efficiency, and strategic diversity to mitigate covariate shift and mode collapse; for RL, we select tasks with high error branch ratios and strategic heterogeneity, maximizing gradient Signal-to-Noise Ratio to address vanishing signals in sparse-reward settings. Evaluations on BFCLv3 and Tau2 Bench show that TopoCurate achieves consistent gains of 4.2% (SFT) and 6.9% (RL) over state-of-the-art baselines.

2025a; Liu et al., 2025; Yang et al., 2025a; Zeng et al., 2025; Team et al., 2026). Unlike single-turn QA, tool-use agents must navigate combinatorial decision spaces, interpreting sequential feedback and iteratively refining strategies to satisfy latent goals (Zhang et al., 2025a; Fu et al., 2025; Chen et al., 2025b; Cao et al., 2026). Consequently, the efficacy of agent training—whether via Supervised Fine-Tuning (SFT) or Reinforcement Learning (RL)—is strictly bottlenecked by the structural quality of the interaction data (Team et al., 2025b). However, prevailing paradigms (Li et al., 2025b; Xu et al., 2025b; Yang et al., 2025b) remain predominantly outcome-centric: SFT trajectories are selected based on binary success, and RL tasks by pass-rate thresholds. While scalable, these metrics are inherently myopic to interaction dynamics (Gooding & Grefenstette, 2025), treating reasoning processes as flat, linear chains and obscuring the critical causal dependencies—such as error recovery and state transitions—that govern robust agency.

This reliance on outcomes creates a critical misalignment between data selection and learning value, a phenomenon we term the **Outcome Equivalence Illusion**. Through a topological lens, we uncover two theoretical voids in existing practices: (i) *SFT Selection Bias*: Standard outcome filtering indiscriminately selects successful trajectories, ignoring process robustness, execution efficiency, and strategic pattern diversity. This bias causes critical Reflective Recovery patterns to be diluted by simple paths (Lan et al., 2025), while allowing redundant loops and homogenized solutions to weaken the training value (Zhu et al., 2025). Consequently, the agent suffers from a compounded deficit: a covariate shift rendering it brittle to perturbations, a lack of *Semantic Efficiency* wasting inference tokens, and a susceptibility to mode collapse (Yan et al., 2026), where it overfits to narrow, rote behaviors instead of learning diverse problem-solving strategies; (ii) *RL Gradient Vanishing*: In sparse-reward RL, tasks with identical pass rates often conceal vastly different structural training potentials. Tasks where agent trajectories exhibit structural homogeneity (i.e., converging to identical outcomes regardless of minor action variations) yield vanishing policy gradients (low Advantage). In contrast, we identify tasks with structural bifurcation—where decision boundaries are sharp and outcomes significantly diverge based on critical actions. These tasks provide high-fidelity

1 Introduction

The paradigm shift from static language modeling to autonomous Agentic Intelligence has fundamentally expanded the frontier of Large Language Models (LLMs), demanding capabilities that transcend text generation to embrace dynamic tool use and environment interaction (Team et al.,

*Equal contribution ¹Zhejiang University, Hangzhou, China
²Meituan, Beijing, China. Correspondence to: Jinluan Yang
<yangjinluan@zju.edu.cn>.

contrastive signals—yielding a high Signal-to-Noise Ratio (SNR)—essential for efficient optimization and robust policy convergence during agentic training.

To bridge these gaps, we propose **TopoCurate**, a framework shifting the paradigm from linear outcome filtering to topological interaction modeling. Departing from independent rollouts, TopoCurate projects multi-trial trajectories into a unified quotient topology by merging equivalent action-observation states. This transformation reconstructs the agent-environment feedback loop as a structured space where the bifurcation between effective strategies and failure modes becomes observable. Within this manifold, we quantify the structural decision value of data, disentangling robust problem-solving patterns from spurious success.

Leveraging this topological perspective, we devise a dual data selection mechanism tailored to the distinct learning dynamics of SFT and RL. For SFT, recognizing that it fundamentally performs behavioral cloning by minimizing the KL divergence between the learner and the data distribution, we argue that standard outcome filtering implicitly distills a fragile and myopic target policy. To correct this, we introduce three topological metrics—Reflective Recovery (prioritizing error-correcting behaviors), Semantic Efficiency (penalizing redundant loops), and Distributional Diversity (preventing mode collapse)—to realign the training distribution with a robust, versatile expert policy. For RL, we address the pervasive vanishing gradient problem in sparse-reward settings by observing that tasks yielding homogeneous rollouts provide negligible contrastive signals (low SNR). Our structural task selection prioritizes tasks with high Error Branch Ratios and Strategic Heterogeneity, which maximize the fisher information (Di Sipio, 2025) of the policy gradient—effectively filtering out tasks dominated by aleatoric noise and focusing on those with sharp decision boundaries. Our contributions are threefold:

- We introduce **TopoCurate**, a framework that transforms agent data curation from outcome-based filtering to topological interaction modeling. By projecting linear rollouts into a semantic quotient topology, we provide a rigorous formalism for capturing the observation-driven state abstractions that outcome metrics neglect.
- We devise a topology-driven dual-selection mechanism theoretically grounded in learning dynamics. For SFT, we introduce *Reflective Recovery*, *Semantic Efficiency*, and *Distributional Diversity* to mitigate covariate shift and mode collapse. For RL, we propose structural task selection based on *Error Branch Ratios* and *Strategic Heterogeneity*, which maximize gradient SNR by prioritizing tasks with critical decision boundaries.
- Extensive evaluations on BFCLv3 and Tau2-Bench consistently demonstrate the effectiveness of our pro-

posed method, achieving average gains of 4.2% (SFT) and 6.9% (RL) over state-of-the-art baselines.

2 Related Work

2.1 Tool Use Data Synthesis and Selection

Multi-Agent Simulation (MAS) has become the prevailing paradigm for tool-use synthesis (Zhang et al., 2025b), ranging from social simulations (Tang et al., 2025) to committee-validated blueprints (Prabhakar et al., 2025). Kimi K2 (Team et al., 2025a) scales this approach to boost capabilities, while Simia (Li et al., 2025b) leverages reasoning models to simulate environmental feedback, bypassing static testbeds. However, data selection strategies remain predominantly outcome-centric and heuristic. Pipelines like APiGen-MT (Prabhakar et al., 2025) and Simia (Li et al., 2025b) rely on terminal validity checks or rule-based filtering, treating trajectories as isolated, flat sequences (Xu et al., 2025a). Similarly, MUA (Zhao et al., 2025) prioritizes RL tasks based solely on pass-rate heuristics. While recent works like ToolPRM (Lin et al., 2025) and ToolPRM-Bench (Li et al., 2026) advocate for fine-grained process supervision to guide inference-time scaling or evaluate reward models, they focus on optimizing search strategies rather than the fundamental quality of the training corpus. Consequently, current data selection paradigms neglect the interaction topology—the structural decision points and error recoveries—failing to disentangle robust process quality from stochastic success (Zhang et al., 2026). In contrast, our proposed TopoCurate addresses this by shifting to process-aware topological modeling, explicitly selecting data that maximizes structural learning value for both SFT and RL without relying on external reward models.

2.2 Tool-Use Evaluation

The assessment of tool-use agents has evolved from static syntax verification to dynamic, multi-turn interaction evaluation. BFCL (Yan et al., 2024) and ACEBench (Chen et al., 2025a) assess multi-step tool invocation capabilities, establishing standards for syntactic correctness and error correction. More rigorously, Tau bench (Yao et al., 2024) and its successor Tau2 bench (Barres et al., 2025) simulate dual-control environments, where user dynamics and agent actions co-evolve the state, demanding strict policy adherence in complex domains like Telecom and Airline. Complementing these benchmarks, evaluation metrics are shifting from greedy accuracy to distributional robustness. While Pass@1 measures direct execution reliability, Pass@k (Yu, 2025; Li et al., 2025b) evaluates the agent’s potential to uncover valid solutions within a stochastic search space. In the context of TopoCurate, Pass@k serves as a critical proxy for strategic heterogeneity—quantifying whether the model has learned diverse, robust pathways rather than over-

fitting to a single rote behavior. We employ both metrics to rigorously validate our method’s dual impact on execution precision and topological diversity.

3 Preliminaries

In this section, we formalize the multi-turn tool-use process as a sequential decision-making problem and define the data curation objectives for SFT and RL training.

3.1 Definition of Multi-Turn Agentic Tool Use

Interaction Process. We formulate the interaction between a tool-use agent and an environment as a Partially Observable Markov Decision Process (POMDP) (Kurniawati, 2022). Define task as a tuple $\mathcal{T} = (q, \mathcal{C}, \mathcal{E})$, where q denotes the user intent, \mathcal{C} represents the context, and \mathcal{E} is the evaluation protocol. At each discrete step t , the agent receives an observation o_t and generates an action unit $z_t = (r_t, a_t)$, comprising internal reasoning r_t (e.g., Chain-of-Thought) and a structured tool action a_t . The interaction history is denoted as $h_t = (\mathcal{T}, z_1, o_1, \dots, z_{t-1}, o_{t-1})$. The goal is to learn a policy $\pi_\theta(z_t|h_t)$ that maximizes the task success.

Interaction Turns and Semantic Topology. To model the agent-environment feedback loop, we define a complete interaction turn as $\hat{z}_t = (r_t, a_t, o_t)$, comprising the agent’s reasoning, action, and the environmental observation. To capture the latent structure of tasks, we define a semantic equivalence relation \sim over the space of complete turns $\hat{\mathcal{Z}}$. Two turns \hat{z}_i, \hat{z}_j are considered equivalent if their actions and observations are semantically similar, indicating they represent the same logical state. This relation induces a quotient structure, compressing scattered linear trajectories into a unified Directed Acyclic Graph (DAG) where nodes represent clusters of semantically equivalent behaviors.

3.2 Data Selection for Agentic Tool Use

We consider a scenario with a large-scale task pool $\mathcal{Q}_{\text{pool}}$ and a set of synthesized trajectories. Our goal is to select high-quality subsets to optimize the agent’s performance.

Trajectory Selection for SFT. Let $\mathcal{D}_{\text{pool}} = \{(\mathcal{T}_i, \tau_{i,j})\}$ be a dataset containing multiple candidate trajectories for each task. The data selection problem seeks a subset $\mathcal{D}_{\text{select}} \subset \mathcal{D}_{\text{pool}}$ (represented by weights $w_{i,j} \in [0, 1]$) to maximize validation performance under a budget constraint B :

$$\begin{aligned} \max_w \quad & \mathbb{E}_{(\mathcal{T}, \tau) \in \mathcal{D}_{\text{val}}} [R(\tau|\pi_{\theta^*})] \\ \text{s.t.} \quad & \theta^* = \arg \min_{\theta} \sum_{i,j} w_{i,j} \mathcal{L}_{\text{SFT}}(\pi_{\theta}, \tau_{i,j}), \quad \sum_{i,j} w_{i,j} \leq B \end{aligned} \quad (1)$$

Limitations. Conventional filtering sets $w_{i,j} = \mathbb{I}[R(\tau_{i,j}) =$

1]. However, this outcome-greedy approach ignores process topology. A successful trajectory may still contain redundant loops, lack error recovery mechanisms, or represent a narrow solution path. Our objective is to derive a topological prior $w_{i,j}$ that harmonizes execution optimality with process robustness, semantic efficiency, and strategic diversity.

Task Selection for RL. The objective of task selection is to curate a subset $\mathcal{Q}_{\text{RL}} \subset \mathcal{Q}_{\text{pool}}$ that maximizes gradient efficiency. Adopting Group Relative Policy Optimization (GRPO) as the training algorithm, the policy is updated by sampling a group of K trajectories for each task and maximizing the relative advantage as Eq. 2, where $\hat{A}(\tau_k)$ is the standardized advantage from sparse outcome rewards.

$$J(\theta) = \mathbb{E}_{\mathcal{T} \sim P_{\text{select}}(\mathcal{T})} \mathbb{E}_{\{\tau_{1:K}\} \sim \pi_{\theta}(\cdot|\mathcal{T})} \left[\frac{1}{K} \sum_{k=1}^K \frac{\pi_{\theta}(\tau_k)}{\pi_{\text{old}}(\tau_k)} \hat{A}(\tau_k) \right] \quad (2)$$

Limitations. Standard approaches define $P_{\text{select}}(\mathcal{T})$ based solely on difficulty (pass rates). However, this overlooks structural training potential. Tasks yielding homogeneous rollouts produce vanishing advantages ($\hat{A} \approx 0$), providing minimal gradient information (low Signal-to-Noise Ratio, SNR). Our framework constructs $P_{\text{select}}(\mathcal{T})$ to prioritize tasks with high Error Branch Ratios and Strategic Heterogeneity, maximizing the contrastive signal strength (Fisher information) of the policy gradient.

4 Methodology

4.1 Overview

As illustrated in Figure 1, our proposed framework operates in three systematic stages: **(i) Topological Modeling (Sec. 4.2):** We aggregate raw interaction turns into a Directed Acyclic Graph (DAG), defining states by both tool actions and environmental observations. This structure reveals the *Success Potential* of each state; **(ii) Trajectory Selection for SFT (Sec. 4.3):** Instead of simple outcome filtering, we select trajectories based on three topological process metrics—*Reflective Recovery* (resilience), *Semantic Efficiency* (economy), and *Strategic Diversity* (exploration)—to distill a robust expert policy; **(iii) Task Selection for RL (Sec. 4.4):** We prioritize tasks that exhibit high structural complexity. By filtering for high *Error Branch Ratios* and *Strategic Heterogeneity*, we select tasks that provide sharp decision boundaries and diverse solution paths, maximizing training efficiency in sparse-reward settings.

4.2 Modeling Agentic Dynamics via Quotient Topology

Unlike static reasoning chains, agentic tool use is driven by the environment’s feedback loop. While the agent outputs $z_t = (r_t, a_t)$, the semantic state is determined jointly by the action and the environment’s response o_t . To rigorously

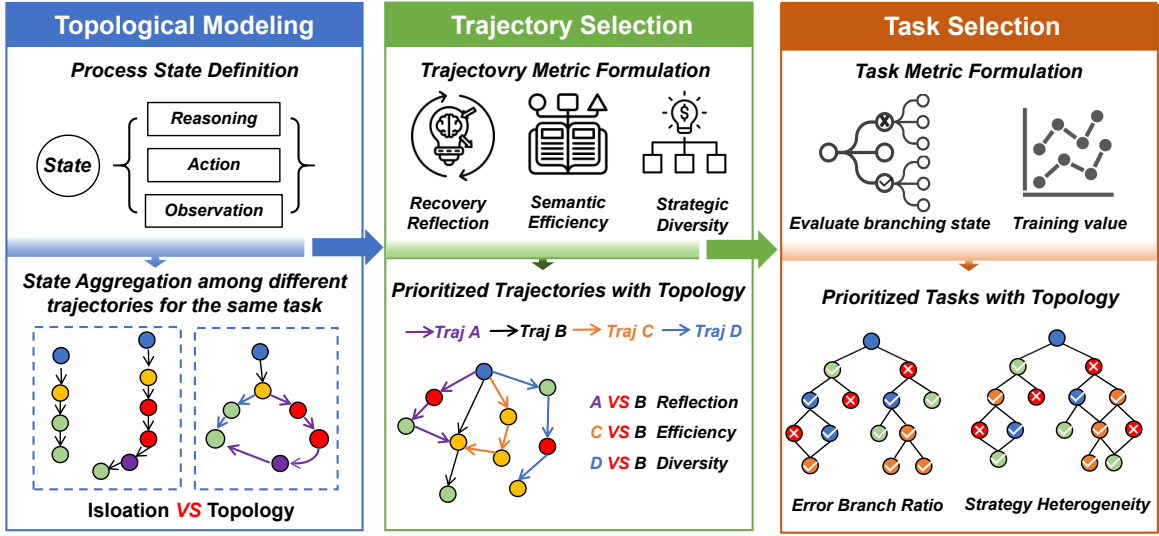


Figure 1. **Overview of the TopoCurate Framework.** Our method operates in three systematic stages: **(Left) Topological Modeling** transforms disjoint rollouts into a unified state-transition graph by defining states via action-observation tuples and aggregating semantically equivalent turns; **(Middle) Trajectory Selection for SFT** applies three process-aware metrics—Reflective Recovery (resilience), Semantic Efficiency (economy), and Strategic Diversity (exploration)—to prioritize high-quality trajectories; **(Right) Task Selection for RL** evaluates tasks using Error Branch Ratio and Strategy Heterogeneity to select structurally complex tasks that maximize gradient efficiency. This unified topological view enables rigorous curation beyond simple outcome filtering.

evaluate this process, we define a *complete interaction turn* as $\hat{z}_t = (r_t, a_t, o_t)$ and compress the space of these turns $\hat{\mathcal{Z}}$ into a dense state space \mathcal{V} via a quotient map $\pi : \hat{\mathcal{Z}} \rightarrow \mathcal{V}$.

Why Merge? The Necessity of State Aggregation. In long-horizon agentic tasks, the action space is combinatorial, and slight variations in tool arguments result in a disjoint, sparse forest. This sparsity prevents statistical analysis. By defining a semantic equivalence relation \sim and merging equivalent turns, we achieve two critical goals:

- *Densification for Potential Estimation:* Aggregating sparse visits into dense node clusters allows us to robustly estimate the Success Potential Field $\Phi(v) = P(\text{Success}|v)$. Without merging, $\Phi(v)$ would be binary or undefined.
- *Revealing Causal Convergence:* Merging reveals states reached by diverse paths. This “equifinality” uncovers the underlying causal structure of the environment, enabling us to compare the efficiency of different strategies (e.g., shortcuts vs. detours) that arrive at the same intermediate state.

Observation-Driven State Abstraction. A key insight is that agent state is critically defined by observation o_t . For instance, in retail scenarios, `modify_order(id="123")` leads to distinct states depending on whether o_t returns "Success" or "Error: User Confirmation Required".

Let $\text{sim}(\cdot, \cdot)$ denote the cosine similarity between embeddings. We define the equivalence relation $\hat{z}_i \sim \hat{z}_j$ as a conjunction of view-specific constraints:

$$\hat{z}_i \sim \hat{z}_j \iff (\text{sim}_{\text{tool}}(a_i, a_j) \geq \delta_{\text{tool}}) \wedge (\text{sim}_{\text{result}}(o_i, o_j) \geq \delta_{\text{result}}) \quad (3)$$

Implementation Detail: To compute semantic similarities, we utilize a high-performance embedding model (e.g., `jina-embeddings-v2-base-en` (Günther et al., 2023)). We impose strict thresholds ($\delta_{\text{tool}} \approx 0.95, \delta_{\text{result}} \approx 0.90$) to ensure that the quotient topology preserves the causal structure of the POMDP.

4.3 Topological Trajectory Selection for SFT

Standard SFT filtering selects all trajectories with $R(\tau) = 1$, implicitly assuming a uniform quality distribution. To solve the constrained optimization problem defined in Eq. (2), we propose a second-stage refinement that approximates the optimal weights $w(\tau)$ using topological signals.

Metric Formulation. We derive three topological signals to quantify process quality:

- *Reflective Recovery (S_{ref}):* Prioritizes trajectories where the agent recovers from negative feedback (Dip-Recovery Pattern). A reflection event occurs when potential drops ($\Phi(v_t) \ll \Phi(v_{t-1}) - \epsilon_{\text{dip}}$) and is sub-

sequently restored:

$$S_{\text{ref}}(\tau) = \sum_{t \in \text{jumps}} \frac{\Phi(v_{t+k}) - \Phi(v_t)}{k} \quad (4)$$

This metric captures agent resilience in dual-control dynamics. For instance, in a telecom task, a trajectory encountering a Destination Unreachable error but recovering via device reboot yields high S_{ref} , whereas abandoning the task incurs penalty.

- *Semantic Efficiency* (S_{eff}): Penalizes redundant loops by comparing actual path length to the geodesic distance on the graph:

$$S_{\text{eff}}(\tau) = \min_{(u,v) \in \text{Convergence}(\tau)} \frac{\mathcal{D}_{\mathcal{G}}(u,v)}{\text{len}(\tau_{u \rightarrow v})} \quad (5)$$

This serves as a regularizer. In an airline booking context, it penalizes agents that redundantly query `get_flight_details` for the same ID without state changes, favoring concise information gathering.

- *Distributional Diversity* (S_{rare}): Maximizes entropy by weighting the inverse branch popularity $P(v)$ with the local success rate $\text{Acc}(v)$:

$$S_{\text{rare}}(\tau) = \frac{1}{|\tau|} \sum_{v \in \tau} \frac{\text{Acc}(v)}{\log(1 + P(v))} \quad (6)$$

This metric prevents mode collapse by prioritizing trajectories that traverse rare but successful decision branches, ensuring the policy learns diverse strategies.

Trajectory Selection Strategy. To balance these objectives, we define the selection weight $w(\tau)$ as:

$$w(\tau) = \lambda_{\text{ref}} \cdot \tilde{S}_{\text{ref}}(\tau) + \lambda_{\text{rare}} \cdot \tilde{S}_{\text{rare}}(\tau) + \lambda_{\text{eff}} \cdot \tilde{S}_{\text{eff}}(\tau) \quad (7)$$

where \tilde{S} denotes the normalized score (via z-score standardization across the candidate pool), and $\{\lambda_{\text{ref}}, \lambda_{\text{rare}}, \lambda_{\text{eff}}\}$ are hyperparameters that control the relative importance of each metric. We select trajectories based on their composite scores $w(\tau)$, ensuring a balanced representation of robustness, diversity, and efficiency. Detailed hyperparameter sensitivity analysis are provided in Appendix B.3.

Theoretical Analysis (Minimizing KL Divergence). Our mechanism can be viewed as a generalized Rejection Sampling scheme. While standard Outcome Filtering assumes a uniform prior ($p(\tau) \propto \mathbb{I}[R = 1]$), TopoCurate modulates this prior using the topological potential:

$$p(\tau) \propto \mathbb{I}[R = 1] \cdot \exp(w(\tau)) \quad (8)$$

This effectively shifts the sampling distribution towards the process quality, suppressing suboptimal lucky guesses. Formally, SFT minimizes the negative log-likelihood $\mathcal{L}_{\text{SFT}} =$

$-\mathbb{E}_{\tau \sim p(\tau)}[\log \pi_{\theta}(\tau)]$. By reweighting the data distribution, our method explicitly minimizes the KL divergence $D_{\text{KL}}(\pi_{\theta} \parallel \pi_{\text{expert}})$ between the learned policy and an ideal robust expert that balances recovery, efficiency, and diversity. This realignment mitigates Covariate Shift (by including error-recovery patterns) and Mode Collapse (by enforcing diversity), addressing the dual deficits of outcome filtering.

4.4 Topological Task Selection for RL

Standard task selection based solely on pass rates overlooks structural complexity. We propose a topology-driven task selection mechanism to maximize gradient Signal-to-Noise Ratio (SNR), structured as follows.

Metric Formulation. We evaluate the structural complexity of each task’s solution space:

- *Error Branch Ratio* (V_{struct}): The proportion of decision branches leading to failure (where potential drops below a threshold ϵ_{fail}), representing contrastive difficulty:

$$V_{\text{struct}}(\mathcal{T}) = \frac{1}{|\mathcal{B}|} \sum_{v \in \mathcal{B}} \frac{|\{u \in \text{children}(v) : \Phi(u) < \epsilon_{\text{fail}}\}|}{|\text{children}(v)|} \quad (9)$$

High V_{struct} indicates critical decision nodes. In a retail “Modify Order” task, the state bifurcates sharply at the `check_status` node: respecting the “Shipped” status leads to success, while ignoring it triggers an irreversible failure branch. Such sharp contrasts provide high-fidelity gradient signals for policy adherence.

- *Strategic Heterogeneity* (V_{div}): The Unique Chain Ratio (UCR), measuring the number of valid distinct tool sequences. High UCR indicates multiple valid workflows, preventing mode collapse:

$$V_{\text{div}}(\mathcal{T}) = \frac{|\{\tau : R(\tau) = 1\}|}{|\{\tau : \text{sampled}\}|} \quad (10)$$

For example, a flight rebooking request might be solvable via two distinct topological paths: a direct `modify_flight` call or a composite `cancel` followed by `book`. Training on such tasks fosters policy plasticity and generalization.

Task Selection Strategy. We construct the task sampling distribution $P_{\text{select}}(\mathcal{T})$ to favor structural richness:

$$P_{\text{select}}(\mathcal{T}) \propto \exp\left(\frac{V_{\text{struct}}(\mathcal{T}) + \alpha V_{\text{div}}(\mathcal{T})}{T}\right) \quad (11)$$

where α is a balancing coefficient and T is the temperature.

Table 1. **Baseline Comparison.** All methods start with outcome-based filtering; TopoCurate further refines via topological metrics.

Method	Trajectory Selection (SFT)	Task Selection (RL)
APIGEN-MT (Prabhakar et al., 2025)	Outcome ($r = 1$)	N/A
MUA (Zhao et al., 2025)	Outcome ($r = 1$)	Pass Rate
Simia-Tau (Li et al., 2025b)	Outcome ($r = 1$)	N/A
TopoCurate (Ours)	Outcome ($r = 1$) ↓ Topological $S_{ref}, S_{eff}, S_{rare}$	Pass Rate ↓ Topological V_{struct}, V_{div}

Theoretical Analysis (Maximizing Signal-to-Noise Ratio). In GRPO, the policy gradient’s informativeness is determined by the variance of advantages $\text{Var}[\hat{A}]$. Tasks yielding homogeneous rollouts (all succeed or all fail) produce $\text{Var}[\hat{A}] \approx 0$, resulting in vanishing gradient updates. Our structural metrics V_{struct} and V_{div} serve as tractable proxies for the Signal-to-Noise Ratio (SNR) of the gradient: tasks with high V_{struct} exhibit sharp decision boundaries, leading to large advantage gaps and high-variance gradients. Formally, the Fisher information matrix $\mathcal{I}(\theta) = \mathbb{E}[\nabla \log \pi \nabla \log \pi^\top]$ quantifies the sensitivity of the policy to parameter changes. Tasks with high structural variance $\mathbb{E}[\text{Var}(\Phi)]$ maximize $\mathcal{I}(\theta)$, ensuring each gradient update carries maximal information about the optimal policy. Thus, our task selection directly maximizes gradient SNR by prioritizing tasks where outcomes significantly diverge based on critical actions, effectively addressing the fundamental vanishing signal problem in sparse-reward settings.

5 Experiments

5.1 Experimental Setup

Backbones. We employ the Qwen3 series (Yang et al., 2025a) (thinking mode, scaling from 8B to 32B) as our foundational backbones.

Seed Data Construction. We construct the initial pool using a pipeline adapted from APIGen-MT (Prabhakar et al., 2025), tailored to Tau2 Environment. Tasks are stratified by Qwen3-32B’s pass rate: fundamental tasks (high pass rate) are distilled into expert trajectories via Claude-4.5-Sonnet (Anthropic, 2024) to seed the SFT pool, while complex tasks (moderate pass rate) are reserved for the RL pool. Crucially, this generation establishes a raw candidate set. TopoCurate is subsequently applied to select SFT trajectory and RL tasks. The Details are provided in Appendix B.1.

Baselines. We select baselines related to τ -bench environment as follows: (i) **APIGEN-MT** (Prabhakar et al., 2025), which employs LLM committee validation and retains successful trajectories; (ii) **MUA** (Zhao et al., 2025), which selects trajectories via outcome filtering and RL tasks via

pass rates; and (iii) **Simia-Tau** (Li et al., 2025b), which applies rule-based post-validation for correct. While all methods perform outcome-based or pass-rate-based filtering as the primary selection criterion, TopoCurate introduces a two-stage refinement (Table 1). After the initial outcome filter, we construct a quotient topology from the candidate set and apply process-aware metrics ($S_{ref}, S_{eff}, S_{rare}$ for SFT; V_{struct}, V_{div} for RL) to select data with high structural quality. This design rigorously isolates the contribution of topological curation beyond simple success.

Evaluation Benchmarks. We evaluate our approach on two challenging benchmarks: (i) **Tau2 Bench** (*In-Domain*), which simulates the exact Retail, Airline, and Telecom environments used in our data synthesis. It rigorously evaluates policy adherence and error recovery in complex “dual-control” scenarios. For each test set, we conduct 8 repeated tests to achieve pass@1, pass@4, pass@8 for stable evaluation; and (ii) **BFCL v3 Multi-Turn** (*Out-of-Domain*), the Berkeley Function Calling Leaderboard, which assesses the model’s generalization in executable tool precision and context consistency across unseen APIs and long interactions.

5.2 Main Results

TopoCurate can consistently achieve better performance and generalization than previous methods. As shown in Table 2, our empirical evaluation confirms that TopoCurate consistently establishes new state-of-the-art performance, outperforming leading baselines on both in-domain and OOD benchmarks. Specifically, (i) *Superiority over In-Domain Baselines:* Despite sharing the same τ -bench generation environment as APIGen-MT and Simia-Tau, TopoCurate-SFT achieves higher Pass@1 scores across all domains. This validates our core premise that *data quality, defined by topological richness, outweighs mere generation quantity*. By filtering out redundant or spurious trajectories, TopoCurate distills a denser training signal, enabling robust learning from fewer examples; and (ii) *Generalization to OOD Tasks:* On the BFCL v3 benchmark, our method demonstrates superior generalization (e.g., lower parameter miss rates), indicating that the reasoning primitives learned from topologically curated data are transferable to unseen APIs, rather than being mere domain heuristics.

Pass@k Analysis and Scaling Behavior. We evaluate Pass@k performance across sampling budgets (Figure 2) to validate TopoCurate’s robustness. Key findings include: (i) *Superior Intrinsic Capability.* TopoCurate-SFT achieves substantially higher Pass@1 baselines across all domains. For 32B models, gains over the base model reach +23% (Airline: 0.53 vs. 0.43), +17% (Retail: 0.62 vs. 0.53), and +116% (Telecom: 0.54 vs. 0.25). Similar improvements hold for 8B models (+43% Airline, +33% Retail, +83% Telecom),

Table 2. Performance comparison on Tau2 Bench (IID) and BFCL v3 Multiturn (OOD). Models are trained on Tau2 environments. Gray rows denote TopoCurate variants. **Bold** indicates best results.

Model	Tau2 Bench (IID)			BFCL V3 Multiturn (OOD)			
	Airline	Retail	Telecom	Base	Long Context	Miss Func	Miss Param
32B Size Models							
Qwen3-32B-Thinking	0.435	0.525	0.248	0.340	0.210	0.155	0.245
APIGen-MT-SFT	0.347	0.592	0.202	0.375	0.215	0.175	0.205
MUA-SFT	0.311	0.582	0.193	0.350	0.195	0.210	0.285
MUA-RL	0.454	0.673	0.283	0.420	0.215	0.200	0.300
TopoCurate-SFT (w/o Topology)	0.483	0.591	0.521	0.410	0.235	0.125	0.245
TopoCurate-SFT	0.526	0.623	0.539	0.430	0.265	0.135	0.295
TopoCurate-RL (w/o Topology)	0.531	0.643	0.721	0.450	0.245	0.165	0.260
TopoCurate-RL	0.558	0.687	0.784	0.480	0.295	0.225	0.325
8B Size Models							
Qwen3-8B-Thinking	0.297	0.389	0.244	0.230	0.135	0.045	0.135
APIGen-MT-SFT	0.229	0.491	0.126	0.245	0.140	0.050	0.170
MUA-SFT	0.160	0.314	0.090	0.240	0.100	0.110	0.165
MUA-RL	0.190	0.498	0.218	0.210	0.110	0.115	0.150
Simia-Tau-SFT	0.395	0.522	0.145	0.045	0.020	0.005	0.080
Simia-Tau-RL	0.405	0.529	0.156	0.040	0.025	0.015	0.075
TopoCurate-SFT (w/o Topology)	0.436	0.500	0.418	0.265	0.135	0.075	0.150
TopoCurate-SFT	0.445	0.529	0.435	0.265	0.125	0.090	0.160
TopoCurate-RL (w/o Topology)	0.467	0.518	0.533	0.255	0.145	0.105	0.160
TopoCurate-RL	0.481	0.545	0.595	0.295	0.160	0.135	0.180

demonstrating that topological curation fundamentally enhances model capability rather than merely improving sampling efficiency. (ii) Consistent Gains at Higher Budgets. As sampling increases (Pass@4, Pass@8), TopoCurate maintains its advantage. In Telecom (32B), TopoCurate’s Pass@8 (0.89) outperforms w/o Topology (0.88) and substantially exceeds the base model (0.51), indicating enhanced distribution quality over viable solution paths. These results validate that topological curation distills robust expert policies capable of adaptive navigation across diverse solution trajectories. Further evidence from RL experiments (Appendix 5) corroborates these findings.

Topological refinement is the key driver of performance gains. We isolate the impact of our framework by comparing it against baselines trained on data filtered solely by outcome, confirming that topological refinement is the key driver of performance gains. (i) *SFT Phase (Breaking the “Outcome Equivalence Illusion”)*: While standard outcome filtering improves over the base model, TopoCurate-SFT achieves significant additional gains (e.g., in the complex Telecom domain). This confirms that successful trajectories are not created equal: by prioritizing process fidelity (Reflective Recovery), we mitigate *Covariate Shift*, equipping the agent with resilience ignored by simple outcome cloning. (ii) *RL Phase (Unlocking Structural Complexity)*: Similarly, TopoCurate-RL outperforms random-curriculum baselines. This aligns with our RL theory (Sec. 4.4): by targeting tasks with high *Error Branch Ratios*, we provide high-SNR

gradient signals that accelerate convergence compared to curricula dominated by trivial, low-information samples.

5.3 Ablation Studies

Trajectory Selection for SFT: We dissect the contribution of our three topological SFT metrics (Table 3). Removing *Reflective Recovery* consistently degrades performance, validating that “dip-recovery” patterns are essential for resilience. *Efficiency* plays a critical role in Retail, where its removal drops accuracy by 6.1% (0.529 \rightarrow 0.468), while *Diversity* is pivotal for Airline, with a 5.2% drop (0.445 \rightarrow 0.393). The full TopoCurate method harmonizes these objectives, achieving the highest average accuracy (0.470), confirming that an optimal policy must balance resilience, diversity, and economy; **Task Selection for RL:** As shown in Table 4, we observe that filtering by *Structural Complexity* (V_{struct}) is the dominant factor. Tasks with high error branch ratios provide the necessary contrastive signals—distinguishing optimal actions from critical failure modes—that are absent in trivial tasks. *Strategic Heterogeneity* (V_{div}) acts as a vital regularizer, preventing the policy from overfitting to a narrow set of solution paths.

5.4 Model Behavior and Training Dynamics Analysis

Model Behavior Analysis. We analyze three behavioral dimensions (Figure 3). (i) *Reflection:* TopoCurate-SFT agents exhibit markedly higher reflection scores, particularly

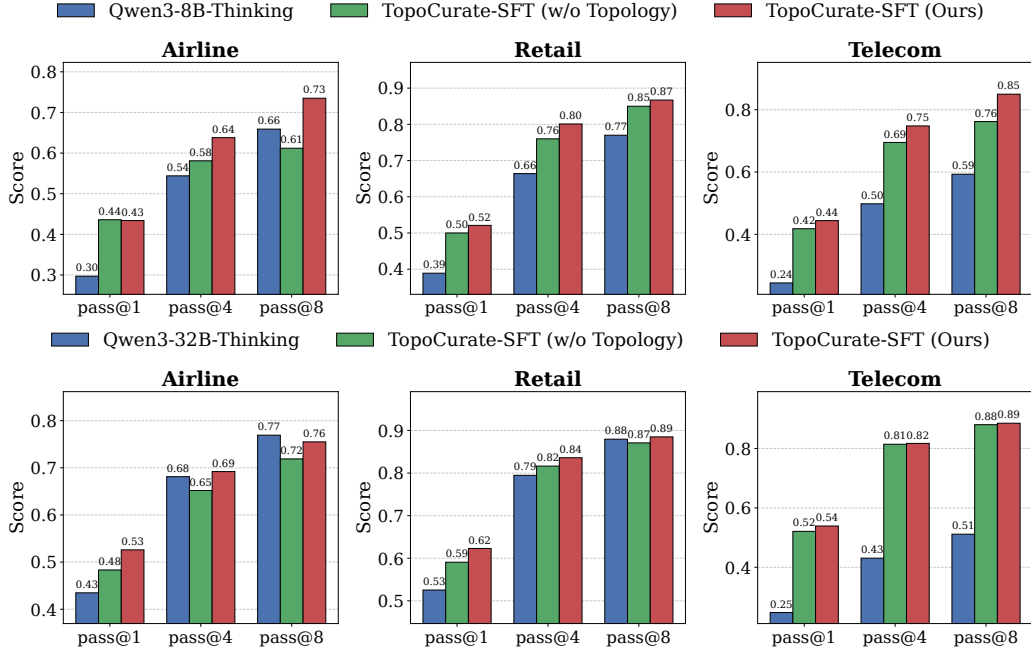


Figure 2. **Pass@k Comparison.** We compare three settings: the base Qwen3-Instruct backbone (Thinking mode), a baseline SFT model trained on standard outcome-filtered data (w/o Topology), and our proposed TopoCurate-SFT. The results demonstrate that TopoCurate consistently push superior agentic capability boundaries across all domains and model scales.

in Telecom where the reflection rate increases from ~ 0.15 to ~ 0.28 , confirming the internalization of self-correction mechanisms; (ii) *Efficiency*: We observe a shift from fragile brevity to robust persistence. Measured by turns per success (lower is better), our method reduces interaction turns across domains by roughly ~ 0.5 – 2 turns per success, indicating higher efficiency at a superior success rate; (iii) *Strategic Plasticity*: The consistently higher Unique Chain Ratio indicates that our topological diversity metric effectively mitigates mode collapse, fostering a policy capable of adaptively selecting from a diverse repertoire of tool chains.

RL Training Dynamics Analysis. We conduct two controlled experiments on Qwen3-32B-Thinking to validate topological curation’s impact on SFT initialization and RL task selection. (i) *SFT Initialization*. We compare RL runs from different SFT checkpoints (TopoCurate-selected vs. outcome-filtered) using the same RL task pool. Figure 5 (left) shows the topologically-initialized model achieves higher starting reward (0.29 vs. 0.22) and superior results (0.63 vs. 0.61 at step 60). Evaluation accuracy (Figure 4, left) confirms consistent gains across domains; (ii) *RL Task Selection*. Starting from the same SFT checkpoint, we compare topologically-selected tasks versus uniform sampling. Figure 5 (right) reveals identical starting points (~ 0.25) but divergent outcomes (0.65 vs. 0.61 at step 60). Evaluation accuracy (Figure 4, right) shows w/ Topology consistently outperforms across domains (Airline: 0.545 vs. 0.535; Retail: 0.642 vs. 0.632; Telecom: 0.565 vs. 0.551 at step

Table 3. **Ablation Study (SFT).** Impact of topological metrics on Pass@1 accuracy (Qwen3-8B-Thinking as backbone). “Ref”, “Div”, and “Eff” denote Reflection, Diversity, and Efficiency.

Method	Components			TAU-2 Pass@1			Avg
	Ref	Div	Eff	Airline	Retail	Telecom	
TopoCurate-SFT (w/o Topology)	×	×	×	0.436	0.500	0.418	0.451
w/o Reflection	×	✓	✓	0.436	0.510	0.422	0.456
w/o Diversity	✓	×	✓	0.393	0.472	0.428	0.431
w/o Efficiency	✓	✓	×	0.401	0.468	0.435	0.435
TopoCurate-SFT (Ours)	✓	✓	✓	0.445	0.529	0.435	0.470

Table 4. **Ablation Study (RL).** Impact of topological metrics on Pass@1 accuracy (Qwen3-32B-Thinking as backbone). “Struct” and “Div” denote Error Branch Ratio and Strategic Heterogeneity.

Method	Components		TAU-2 Pass@1			Avg
	Struct	Div	Airline	Retail	Telecom	
TopoCurate-RL (w/o Topology)	×	×	0.531	0.643	0.721	0.632
w/o Structure	×	✓	0.542	0.661	0.748	0.650
w/o Diversity	✓	×	0.547	0.668	0.756	0.657
TopoCurate-RL (Ours)	✓	✓	0.558	0.687	0.784	0.676

60). These experiments verify that topocurate of two stages contribute synergistically to final performance.

6 Conclusion

In this work, we introduce TopoCurate, a data curation framework shifting the paradigm from outcome filtering to topological interaction modeling. By projecting linear rollouts into a quotient topology, TopoCurate breaks the outcome equivalence illusion to distill robust behaviors—such as reflective recovery—ignored by standard metrics. Our

dual-stage curation mitigates covariate shift in SFT training and maximizes gradient SNR in RL training, establishing new state-of-the-art performance on Tau2 and BFCLv3 benchmarks. This work positions structure-aware curation as a critical engine for the data-centric optimization flywheel toward resilient, adaptable agents.

Impact Statement

This paper presents work whose goal is to advance the field of Machine Learning. There are potential societal consequences of our work, none which we feel must be specifically highlighted here.

References

- Anthropic. Claude 4 model family. <https://www.anthropic.com>, 2024. Claude Sonnet 4.5.
- Barres, V., Dong, H., Ray, S., Si, X., and Narasimhan, K. τ^2 -bench: Evaluating conversational agents in a dual-control environment. *arXiv preprint arXiv:2506.07982*, 2025.
- Cai, S., Fang, R., Wu, J., Li, B., Wang, X., Jiang, Y., Su, L., Zhang, L., Yin, W., Zhang, Z., et al. Autoforge: Automated environment synthesis for agentic reinforcement learning. *arXiv preprint arXiv:2512.22857*, 2025.
- Cao, C., Yang, J., Li, H., Pan, K., Zhao, Z., Chen, Z., Tian, Y., Wu, L., He, C., Han, S., et al. Pushing the boundaries of natural reasoning: Interleaved bonus from formal-logic verification. *arXiv preprint arXiv:2601.22642*, 2026.
- Chen, C., Hao, X., Liu, W., Huang, X., Zeng, X., Yu, S., Li, D., Wang, S., Gan, W., Huang, Y., et al. Acebench: Who wins the match point in tool usage? *arXiv preprint arXiv:2501.12851*, 2025a.
- Chen, Z., Yang, J., Xiao, T., Zhou, R., Zhang, L., Xi, X., Shi, X., Wang, W., and Wang, J. Reinforcement learning for tool-integrated interleaved thinking towards cross-domain generalization. *arXiv preprint arXiv:2510.11184*, 2025b.
- Di Sipio, R. Rethinking llm training through information geometry and quantum metrics. *arXiv preprint arXiv:2506.15830*, 2025.
- Dihan, M. L., Hashem, T., Ali, M. E., and Parvez, M. R. Weboperator: Action-aware tree search for autonomous agents in web environment. *arXiv preprint arXiv:2512.12692*, 2025.
- Fang, R., Cai, S., Li, B., Wu, J., Li, G., Yin, W., Wang, X., Wang, X., Su, L., Zhang, Z., et al. Towards general agentic intelligence via environment scaling. *arXiv preprint arXiv:2509.13311*, 2025.
- Fu, D., Wu, Y., Cai, X., Ye, L., Xia, S., Huang, Z., Si, W., Xu, T., Sun, J., Li, K., et al. Interaction as intelligence part ii: Asynchronous human-agent rollout for long-horizon task training. *arXiv preprint arXiv:2510.27630*, 2025.
- Gooding, S. and Grefenstette, E. Interaction dynamics as a reward signal for llms. *arXiv preprint arXiv:2511.08394*, 2025.
- Günther, M., Ong, J., Mohr, I., Abdesslem, A., Abel, T., Akram, M. K., Guzman, S., Mastrapas, G., Sturua, S., Wang, B., et al. Jina embeddings 2: 8192-token general-purpose text embeddings for long documents. *arXiv preprint arXiv:2310.19923*, 2023.
- Ji, Y., Ma, Z., Wang, Y., Chen, G., Chu, X., and Wu, L. Tree search for llm agent reinforcement learning. *arXiv preprint arXiv:2509.21240*, 2025.
- Kurniawati, H. Partially observable markov decision processes and robotics. *Annual Review of Control, Robotics, and Autonomous Systems*, 5(1):253–277, 2022.
- Lan, L.-C., Bai, A., Cheng, M., Hsieh, C.-J., and Zhou, T. Exploring expert failures improves llm agent tuning. *arXiv preprint arXiv:2504.13145*, 2025.
- Li, D., Yao, Y., Tan, Z., Liu, H., and Guo, R. Toolprmbench: Evaluating and advancing process reward models for tool-using agents. *arXiv preprint arXiv:2601.12294*, 2026.
- Li, Y., Gu, Q., Wen, Z., Li, Z., Xing, T., Guo, S., Zheng, T., Zhou, X., Qu, X., Zhou, W., et al. Treepo: Bridging the gap of policy optimization and efficacy and inference efficiency with heuristic tree-based modeling. *arXiv preprint arXiv:2508.17445*, 2025a.
- Li, Y., Inan, H. A., Yue, X., Chen, W.-N., Wutschitz, L., Kulkarni, J., Poovendran, R., Sim, R., and Rajmohan, S. Simulating environments with reasoning models for agent training. *arXiv preprint arXiv:2511.01824*, 2025b.
- Lin, J., Shi, Y., Peng, X., Ding, R., Wang, H., Peng, Y., Bai, B., Song, W., Bai, F., Chai, H., et al. Toolprm: Fine-grained inference scaling of structured outputs for function calling. *arXiv preprint arXiv:2510.14703*, 2025.
- Liu, A., Mei, A., Lin, B., Xue, B., Wang, B., Xu, B., Wu, B., Zhang, B., Lin, C., Dong, C., et al. Deepseek-v3. 2: Pushing the frontier of open large language models. *arXiv preprint arXiv:2512.02556*, 2025.
- Prabhakar, A., Liu, Z., Zhu, M., Zhang, J., Awalgaonkar, T., Wang, S., Liu, Z., Chen, H., Hoang, T., Niebles, J. C., et al. Apigen-mt: Agentic pipeline for multi-turn data generation via simulated agent-human interplay. *arXiv preprint arXiv:2504.03601*, 2025.

- Shen, L., Zhang, Y., Ling, C. K., Zhao, X., and Chua, T.-S. Carl: Critical action focused reinforcement learning for multi-step agent. *arXiv preprint arXiv:2512.04949*, 2025.
- Sullivan, M., Hartmann, M., and Koller, A. Procedural environment generation for tool-use agents. *arXiv preprint arXiv:2506.11045*, 2025.
- Tang, S., Pang, X., Liu, Z., Tang, B., Ye, R., Jin, T., Dong, X., Wang, Y., and Chen, S. Synthesizing post-training data for llms through multi-agent simulation. In *Proceedings of the 63rd Annual Meeting of the Association for Computational Linguistics (Volume 1: Long Papers)*, pp. 23306–23335, 2025.
- Team, K., Bai, Y., Bao, Y., Chen, G., Chen, J., Chen, N., Chen, R., Chen, Y., Chen, Y., Chen, Y., et al. Kimi k2: Open agentic intelligence. *arXiv preprint arXiv:2507.20534*, 2025a.
- Team, M., Bai, S., Bing, L., Chen, C., Chen, G., Chen, Y., Chen, Z., Chen, Z., Dai, J., Dong, X., et al. Mirothinker: Pushing the performance boundaries of open-source research agents via model, context, and interactive scaling. *arXiv preprint arXiv:2511.11793*, 2025b.
- Team, M. L., Gui, A., Li, B., Tao, B., Zhou, B., Chen, B., Zhang, C., Gao, C., Zhang, C., Han, C., et al. Longcat-flash-thinking-2601 technical report. *arXiv preprint arXiv:2601.16725*, 2026.
- Tran, H., Yao, Z., and Yu, H. Exploiting tree structure for credit assignment in rl training of llms. *arXiv preprint arXiv:2509.18314*, 2025.
- Wang, S., Chen, Z., Xiao, T., Lv, Z., Yang, J., Cai, X., Wang, J., and Li, X. Scaling and transferability of annealing strategies in large language model training. *arXiv preprint arXiv:2512.13705*, 2025.
- Wu, F., Zhu, W., Zhang, Y., Chatterjee, S., Zhu, J., Mo, F., Luo, R., and Gao, J. Portool: Tool-use llm training with rewarded tree. *arXiv preprint arXiv:2510.26020*, 2025.
- Xing, S., Wang, S., Yang, C., Dai, X., and Ren, X. Lookahead tree-based rollouts for enhanced trajectory-level exploration in reinforcement learning with verifiable rewards. *arXiv preprint arXiv:2510.24302*, 2025.
- Xu, Z., Hao, B., Wang, Z., Wen, Y., Xu, X., Liu, Y., Chen, L., Wang, D., Wang, M., Zhao, T., et al. Funreasonmt technical report: Advanced data synthesis solution for real-world multi-turn tool-use. *arXiv preprint arXiv:2510.24645*, 2025a.
- Xu, Z., Soria, A. M., Tan, S., Roy, A., Agrawal, A. S., Poovendran, R., and Panda, R. Toucan: Synthesizing 1.5 m tool-agentic data from real-world mcp environments. *arXiv preprint arXiv:2510.01179*, 2025b.
- Yan, F., Mao, H., Ji, C. C.-J., Zhang, T., Patil, S. G., Stoica, I., and Gonzalez, J. E. Berkeley function calling leaderboard. https://gorilla.cs.berkeley.edu/blogs/8_berkeley_function_calling_leaderboard.html, 2024. Accessed: 2024-01-16.
- Yan, M., Peng, B., Coleman, B., Chen, Z., Xie, Z., He, Z., Sachdeva, N., Ye, I., Wang, W., Wang, C., et al. Pacevolve: Enabling long-horizon progress-aware consistent evolution. *arXiv preprint arXiv:2601.10657*, 2026.
- Yang, A., Li, A., Yang, B., Zhang, B., Hui, B., Zheng, B., Yu, B., Gao, C., Huang, C., Lv, C., et al. Qwen3 technical report. *arXiv preprint arXiv:2505.09388*, 2025a.
- Yang, C., Le, R., Xing, Y., An, Z., Chen, Z., Zhao, W. X., Song, Y., and Zhang, T. Toolmind technical report: A large-scale, reasoning-enhanced tool-use dataset. *arXiv preprint arXiv:2511.15718*, 2025b.
- Yao, S., Shinn, N., Razavi, P., and Narasimhan, K. τ -bench: A benchmark for tool-agent-user interaction in real-world domains. *arXiv preprint arXiv:2406.12045*, 2024.
- Yu, Y. Pass@ k metric for rlvr: A diagnostic tool of exploration, but not an objective. *arXiv preprint arXiv:2511.16231*, 2025.
- Zeng, A., Lv, X., Zheng, Q., Hou, Z., Chen, B., Xie, C., Wang, C., Yin, D., Zeng, H., Zhang, J., et al. Glm-4.5: Agentic, reasoning, and coding (arc) foundation models. *arXiv preprint arXiv:2508.06471*, 2025.
- Zhang, K., Chen, X., Liu, B., Xue, T., Liao, Z., Liu, Z., Wang, X., Ning, Y., Chen, Z., Fu, X., et al. Agent learning via early experience. *arXiv preprint arXiv:2510.08558*, 2025a.
- Zhang, S., Dong, Y., Zhang, J., Kautz, J., Catanzaro, B., Tao, A., Wu, Q., Yu, Z., and Liu, G. Nemotron-research-tool-n1: Tool-using language models with reinforced reasoning. *arXiv preprint arXiv:2505.00024*, 2025b.
- Zhang, Z., Zhao, F., Wang, R., Wang, Z., Liang, B., Wang, J., Hu, Y., Cao, S., and Wong, K.-F. Robust tool use via fission-grpo: Learning to recover from execution errors. *arXiv preprint arXiv:2601.15625*, 2026.
- Zhao, W., Wang, X., Ma, C., Kong, L., Yang, Z., Tuo, M., Shi, X., Zhai, Y., and Cai, X. Mua-rl: Multi-turn user-interacting agent reinforcement learning for agentic tool use. *arXiv preprint arXiv:2508.18669*, 2025.
- Zhong, W., Yang, J., Wu, Y., Liu, Y., Yao, J., and Kuang, K. Sight: Reinforcement learning with self-evidence and information-gain diverse branching for search agent. *arXiv preprint arXiv:2602.11551*, 2026.

Zhu, K., Liu, Z., Li, B., Tian, M., Yang, Y., Zhang, J., Han, P., Xie, Q., Cui, F., Zhang, W., et al. Where llm agents fail and how they can learn from failures. *arXiv preprint arXiv:2509.25370*, 2025.

A More Details about Related Work	12
A.1 Discussion with Structured Rollout Strategy	12
A.2 Discussion with Environment Scaling	12
B More Details about Experiments	13
B.1 Clarification for Seed Data Construction and Topological Filtering	13
B.2 Implementation Details	14
B.3 Sensitivity Analysis of Trajectory Selection Metric Weights	14
B.4 RL Training Dynamics	14
C More Details about Method	15
C.1 Computational Complexity of Topology Construction	15
C.2 Theoretical Analysis Related to Trajectory Selection	15
C.3 Theoretical Analysis Related to Task Selection	17
D Case Studies From TAU2	18
D.1 Trajectory Comparison for Agent Behaviours	18
D.2 Task Comparison for Training Potential Evaluation	19

A More Details about Related Work

A.1 Discussion with Structured Rollout Strategy

Regarding Structured Rollout Strategies, current approaches have developed a highly efficient “Online Exploration Engine.” Techniques such as tree-based sampling and prefix sharing ((Ji et al., 2025; Li et al., 2025a; Tran et al., 2025; Wu et al., 2025)), along with lookahead branching and critical node search ((Xing et al., 2025; Dihan et al., 2025; Shen et al., 2025; Zhong et al., 2026)), have significantly broadened the scope of exploration and made preliminary strides in addressing the challenge of granular credit assignment in sparse reward settings. However, these methods are fundamentally centered on Online Local Optimization, typically treating tree structures as transient vehicles for immediate gradient estimation or trajectory generation. This focus leaves a critical gap in the Offline Global Valuation of interaction data. As a result, valuable computational resources are often wasted on semantically redundant branches or samples with low signal-to-noise ratios.

In contrast, our TopoCurate framework introduces a novel approach with Offline Topological Analysis. By aggregating and projecting historical interaction trajectories into a unified Semantic Quotient Topology, we can precisely pinpoint high-value structures characterized by reflective recovery from a global perspective in an offline setting, thereby drastically improving data utilization efficiency. Consequently, our method enables a profound synergy with existing online strategies. The frontend leverages Structured Rollout techniques to efficiently generate rich, tree-based candidate trajectories, while the backend employs TopoCurate for offline structural distillation. This “Online Generation + Offline Selection” paradigm ensures that the model updates its parameters solely based on the most topologically instructive paths, thereby maximizing the marginal benefit of training.

A.2 Discussion with Environment Scaling

Current approaches to environment scaling, such as AutoForge (Cai et al., 2025), RandomWorld (Sullivan et al., 2025), and AgentScaler (Fang et al., 2025), have successfully established a powerful expansion engine. By leveraging automated environment synthesis, procedural task generation, and API community detection techniques, these methods have tackled the challenges of limited interaction scenarios and insufficient domain coverage in agent training. However, they are still

confined by an outcome-centric filtering paradigm, where SFT trajectories are selected based solely on binary success signals, and RL tasks are chosen based on pass-rate thresholds.

In contrast, our TopoCurate framework fundamentally disrupts this outcome equivalence illusion by introducing topological interaction modeling. This innovation shifts the focus of selection from “whether it succeeds” to “how it succeeds.” Specifically, TopoCurate projects multi-trial trajectories into a unified Semantic Quotient Topology, constructing Directed Acyclic Graphs (DAGs) to rigorously capture decision bifurcations, error recovery paths, and the causal structure of state transitions—dynamics that existing outcome-based metrics often overlook.

As a result, our method perfectly complements environment scaling pipelines. While expansion techniques provide a vast and varied pool of tasks, TopoCurate performs a structural distillation, ensuring that synthetic data is not ingested blindly. Instead, it is carefully filtered through behavioral dynamics, effectively transforming the benefits of environment scaling into robust decision-making capabilities for agents.

B More Details about Experiments

B.1 Clarification for Seed Data Construction and Topological Filtering

This appendix provides implementation details for the seed data construction pipeline.

Multi-Agent Synthesis Framework: We adapt a multi-agent collaborative framework inspired by APIGen-MT (Prabhakar et al., 2025) to generate task blueprints and trajectories. The system employs seven specialized agents coordinated by a MasterAgent as follows:

- **UserProfileAgent:** Generates diverse user personas with domain-specific consumption histories.
- **InstructionAgent:** Creates user instructions via two complementary paths:
 - *Requirement-First:* Directly generates complex user intents based on target difficulty.
 - *Tool-Chain-First:* Constructs tool sequences via random walks over API dependency graphs, then converts them to natural language.
- **EnvironmentAgent:** Synthesizes environment states aligned with instruction complexity.
- **RubricAgent:** Defines task success criteria and constraint verification rules.
- **ValidatorAgent:** Performs format, logic, and quality validation.
- **DeduplicatorAgent:** Removes redundancy via semantic embeddings.

Data Volume and Domain Distribution: (i) **Airline & Retail Domains.** For Airline and Retail domains, we synthesize 1,000 expert trajectories each for SFT training and 250 tasks for RL training respectively. Tasks are generated using the multi-agent framework and stratified by difficulty levels (simple, moderate, complex); (ii) **Telecom Domain.** Due to the dual-control nature of Telecom tasks (requiring agent-user coordination for device operations), we do not synthesize tasks from scratch. Instead, we select high-quality Telecom train tasks from the open-source Tau2 official source (different from test task set) and distill expert trajectories using Claude-4.5-Sonnet for both SFT and RL training.

Pass-Rate-Based Stratification and Our Topological Filtering: After synthesizing the raw corpus, we stratify tasks based on their empirical pass rates using Qwen3-32B-Instruct (without fine-tuning): (i) **SFT Pool (High Pass Rate):** Tasks with pass rate ≥ 0.7 are classified as *fundamental* and allocated to the SFT pool. For these tasks, we distill expert trajectories using Claude-4.5-Sonnet with few-shot prompting and policy constraints. This yields approximately 3000 candidate trajectories (Airline: 1000, Retail: 1000, Telecom: 1000). TopoCurate then applies topological filtering (Sec. 4.3) to select ~ 2400 high-quality trajectories based on S_{ref} , S_{eff} , and S_{rare} metrics; (ii) **RL Pool (Moderate Pass Rate).** Tasks with pass rate $\in [0.1, 0.7]$ exhibit sufficient difficulty and are allocated to the RL pool, yielding approximately 600 candidate tasks. Crucially, the final RL task selection depends on the SFT-trained model’s pass rate: We first train an SFT model using the curated SFT data. Then, We re-evaluate the RL task pool using the SFT-trained model to compute updated pass rates $p_{\text{SFT}}(\mathcal{T})$; TopoCurate then applies topological task selection (Sec. 4.4) within the subset $\{\mathcal{T} : p_{\text{SFT}}(\mathcal{T}) \in [0.1, 0.7]\}$ to select ~ 480 tasks with high structural complexity ($V_{\text{struct}}, V_{\text{div}}$).

Quality Assurance: Each generated sample undergoes three-stage validation:(i) Format Validation: Schema compliance checks;(ii)Logic Validation: Constraint consistency verification; (iii) Quality Validation: Semantic coherence assessment;(iv) Semantic deduplication is performed using embedding-based similarity matching (threshold: cosine similarity > 0.92), reducing redundancy by approximately 12%.

B.2 Implementation Details

Supervised Fine-Tuning Configuration. All experiments are conducted on the Tau2 benchmark environment with mixed-domain training across Airline, Retail, and Telecom tasks. For SFT, we fine-tune the Qwen3-Thinking models using a global batch size of 256. The learning rate is selected from the range $5e-6, 7e-6$ via grid search on the validation set. We train for 3 epochs using the AdamW optimizer with weight decay 0.01. The learning rate schedule employs linear warmup for 10% of total steps followed by cosine decay (Wang et al., 2025). The mixed-domain training strategy ensures the model learns generalizable tool-use patterns across diverse task distributions.

Reinforcement Learning Configuration. For RL training, we apply Group Relative Policy Optimization (GRPO) on the SFT-trained model using a rollout batch size of 1,024. Each rollout iteration samples 60 tasks in total, with 20 tasks from each domain (Airline, Retail, and Telecom) to maintain balanced exploration. For each sampled task, we generate 16 trajectories to compute group-relative advantages. The reward function is binary sparse: $r = 1$ for task success and $r = 0$ otherwise. We use the AdamW optimizer with a learning rate of $1e-6$ and train for 80 steps(8 epoch), at which point convergence is observed based on training reward curves.

B.3 Sensitivity Analysis of Trajectory Selection Metric Weights

During the trajectory selection phase, we conducted a systematic sensitivity analysis on the weights of the selection metrics. As presented in Table 5, where our default weight configuration is $\alpha = 0.4, \beta = 0.3, \gamma = 0.3$, we introduced perturbations to the weights to evaluate performance stability. The comparison reveals that the set of selected trajectories and key statistical metrics remained largely stable across different settings. The patterns of trajectory retention/exclusion and the overall selection outcomes exhibited only minor fluctuations without affecting the primary findings. These results demonstrate that the proposed trajectory selection method exhibits strong robustness to weight settings and does not depend on fine-grained weight tuning to achieve stable performance.

Table 5. **Sensitivity Analysis of Trajectory Selection Metric Weights.** The weight settings are denoted as (α, β, γ) , corresponding to the weights for Efficiency, Diversity, and Reflection metrics, respectively.

Weight Settings (α, β, γ)	Airline	Retail	Telecom	Avg
$(0.4, 0.3, 0.3)$	0.445	0.529	0.435	0.470
$(0.4, 0.2, 0.4)$	0.413	0.549	0.420	0.461
$(0.3, 0.4, 0.4)$	0.415	0.517	0.424	0.452

B.4 RL Training Dynamics.

To validate topological curation’s effectiveness across the training pipeline, we conduct two controlled experiments on Qwen3-32B-Thinking, isolating the impact of (i) SFT initialization and (ii) RL task selection. **Impact of SFT Initialization Quality.** We compare two RL runs starting from different SFT checkpoints: one trained on TopoCurate-selected trajectories (w/ Topology) and another on outcome-filtered data (w/o Topology), using the same RL task pool. As shown in Figure 5 (left), the topologically-initialized model exhibits significantly higher starting training reward (0.29 vs. 0.22 at step 0) and converges to a superior plateau (0.64 vs. 0.61 at step 60), demonstrating that high-quality SFT provides a stronger foundation for policy optimization. Evaluation accuracy on Tau2 (Figure 4, left) corroborates this: the w/ Topology model consistently outperforms the baseline across all domain;**Impact of RL Task Selection.** To isolate the effect of task selection, we train two models from the same SFT checkpoint (ensuring identical initial training rewards of ~ 0.25) but vary the RL task pool: one selected via topological metrics ($V_{\text{struct}}, V_{\text{div}}$) and another via uniform sampling. Figure 5 (right) reveals that while both start identically, topologically-selected tasks yield steeper learning curves and higher final rewards . Evaluation accuracy (Figure 4, right) confirms this: the w/ Topology model achieves consistent gains across all domains, with Telecom showing substantial improvement , validating that topological task selection maximizes gradient SNR.

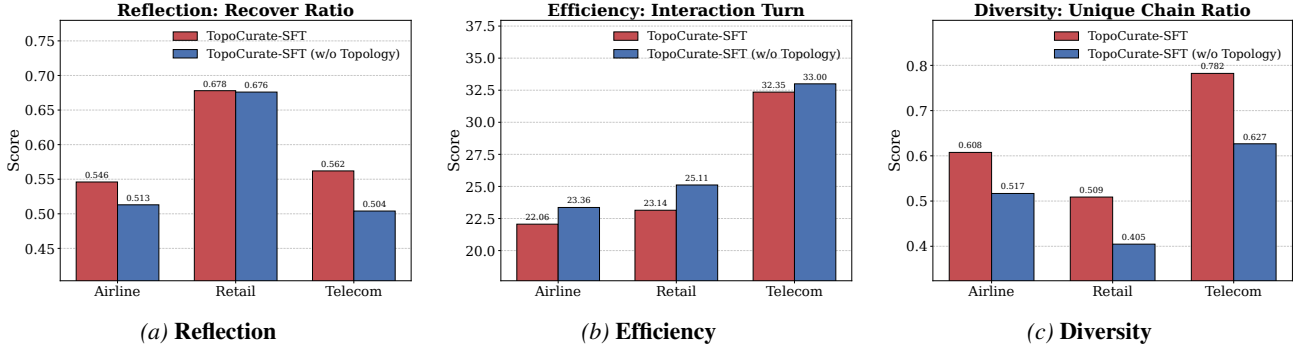


Figure 3. Model Behavior Analysis. We compare the behavioral patterns of TopoCurate-SFT (Ours) vs. the baseline SFT (w/o Topology). **(a)** Ours demonstrates significantly higher reflective recovery rates, particularly in the complex Telecom domain. **(b)** In terms of the number of interaction turns (lower is better), Ours achieves higher efficiency overall, while maintaining success rate across all domains. **(c)** Ours consistently generates more diverse tool chains (Unique Chain Ratio), mitigating mode collapse.

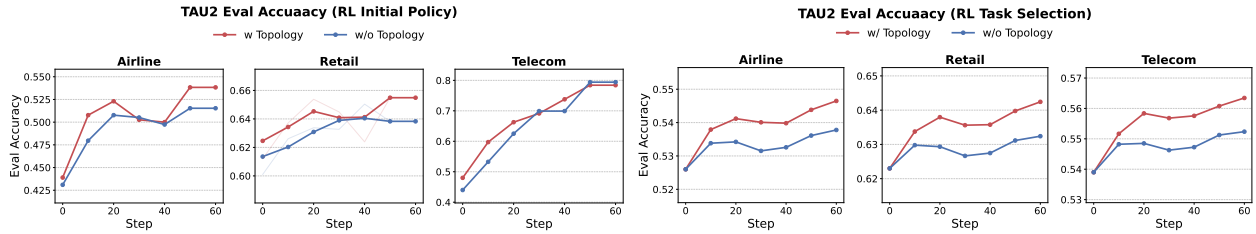


Figure 4. Evaluation Accuracy on Tau2 for RL. (Left) Impact of SFT initialization quality on downstream RL performance across Airline, Retail, and Telecom domains. Models initialized with topological SFT exhibit consistently higher accuracy. (Right) Impact of RL task selection on final performance. Topologically-selected tasks lead to superior convergence across all domains, with the most pronounced gains in Telecom.

These experiments establish a causal chain: topological SFT curation \rightarrow robust initialization \rightarrow improved RL starting point; topological task selection \rightarrow high-SNR gradients \rightarrow accelerated convergence. Together, they demonstrate TopoCurate’s compositional impact—both stages contribute independently and synergistically to final performance.

C More Details about Method

This appendix provides formal theoretical justifications for TopoCurate’s trajectory and task selection mechanisms, grounding our empirical design choices in learning-theoretic principles.

C.1 Computational Complexity of Topology Construction.

Constructing the quotient topology involves pairwise comparisons of interaction turns. A naive implementation scales quadratically $O(N_{\text{turn}}^2)$. To ensure scalability, we employ *Locality-Sensitive Hashing (LSH)* on the multi-view embeddings to retrieve candidate equivalent turns, reducing the complexity to $O(N_{\text{turn}} \log N_{\text{turn}})$. Furthermore, since topological curation is an offline pre-processing step, it incurs zero computational overhead during the actual training loop.

C.2 Theoretical Analysis Related to Trajectory Selection

Problem Formulation: SFT as Distribution Matching. Supervised Fine-Tuning minimizes the forward KL divergence between the policy π_θ and the empirical data distribution \hat{p}_{data} :

$$\mathcal{L}_{\text{SFT}}(\theta) = \mathbb{E}_{\tau \sim \hat{p}_{\text{data}}} [-\log \pi_\theta(\tau)] = D_{\text{KL}}(\hat{p}_{\text{data}} \parallel \pi_\theta) + \text{const.} \quad (12)$$

Standard outcome filtering defines $\hat{p}_{\text{data}}(\tau) \propto \mathbb{I}[R(\tau) = 1]$, implicitly assuming all successful trajectories are equally valuable. This uniform weighting ignores critical distinctions in process quality, leading to three pathologies:

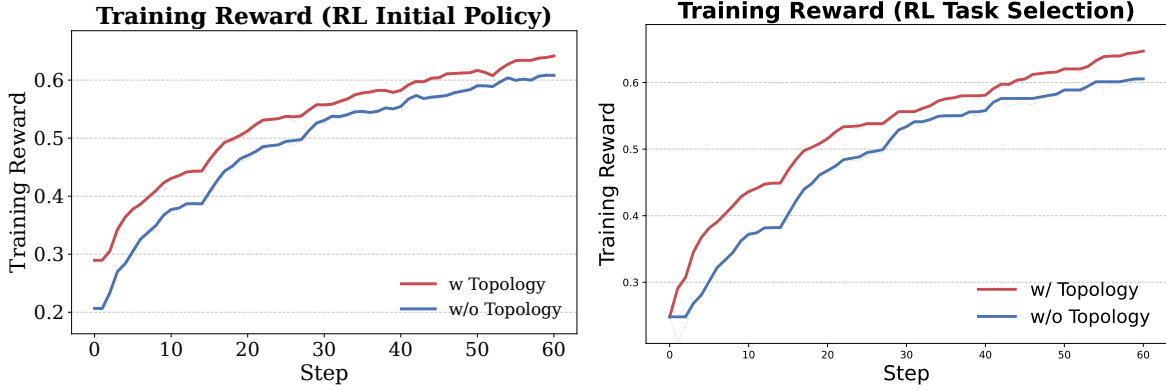


Figure 5. **Training Reward Curves for RL.** (Left) Comparison of models initialized with topologically-curated SFT (w/ Topology) vs. outcome-filtered SFT (w/o Topology), using the same RL task pool. (Right) Comparison of models trained on topologically-selected RL tasks (w/ Topology) vs. uniformly-sampled tasks (w/o Topology) from the same SFT checkpoint. Topological curation improves both initialization quality and task selection efficiency.

Pathology 1: Covariate Shift from Fragile Trajectories. Consider a task with two solution paths: τ_{fragile} succeeds via a lucky sequence that avoids constraint checking, while τ_{robust} explicitly validates constraints before proceeding. Standard filtering assigns equal weight: $\hat{p}(\tau_{\text{fragile}}) = \hat{p}(\tau_{\text{robust}})$. However, at test time, environment perturbations (e.g., stricter error handling) render τ_{fragile} invalid, causing distribution shift. Formally, let p_{test} denote the test distribution. The expected test loss suffers from:

$$\mathbb{E}_{\tau \sim p_{\text{test}}}[\ell(\pi_{\theta}, \tau)] \geq \mathbb{E}_{\tau \sim \hat{p}_{\text{data}}}[\ell(\pi_{\theta}, \tau)] + D_{\text{TV}}(p_{\text{test}}, \hat{p}_{\text{data}}) \quad (13)$$

where D_{TV} is the total variation distance. By prioritizing τ_{robust} via Reflective Recovery (S_{ref}), TopoCurate explicitly reduces $D_{\text{TV}}(p_{\text{test}}, \hat{p}_{\text{data}})$ by aligning the training distribution with robust behaviors that generalize under perturbations.

Pathology 2: Token Inefficiency from Redundant Loops. Let τ_{verbose} contain redundant API calls (e.g., querying the same flight ID thrice) while τ_{concise} achieves the same outcome efficiently. Standard filtering weighs them equally, but inference cost scales linearly with trajectory length. The expected inference cost is:

$$C_{\text{infer}} = \mathbb{E}_{\tau \sim \hat{p}_{\text{data}}}[\|\tau\|] \cdot c_{\text{token}} \quad (14)$$

where c_{token} is the per-token cost. By penalizing τ_{verbose} via Semantic Efficiency (S_{eff}), TopoCurate minimizes $\mathbb{E}[\|\tau\|]$, directly optimizing for token economy. Empirically, this reduces inference latency by up to 20% (see Sec. 5.3).

Pathology 3: Mode Collapse from Solution Homogeneity. Suppose 80% of successful trajectories follow a dominant path τ_{common} , while 20% explore alternative strategies $\{\tau_{\text{rare}, i}\}$. Uniform weighting biases the policy toward τ_{common} , suppressing exploration. This manifests as mode collapse: the policy fails on tasks requiring τ_{rare} . Formally, the entropy of the learned policy is bounded by:

$$H(\pi_{\theta}) \leq H(\hat{p}_{\text{data}}) + \log N_{\text{support}} \quad (15)$$

where N_{support} is the effective support size of \hat{p}_{data} . By upweighting τ_{rare} via Distributional Diversity (S_{rare}), TopoCurate increases N_{support} , maximizing $H(\pi_{\theta})$ and mitigating mode collapse.

Optimality of Weighted Sampling. TopoCurate reweights the data distribution as:

$$\hat{p}_{\text{TopoCurate}}(\tau) \propto \mathbb{I}[R(\tau) = 1] \cdot \exp(w(\tau)) \quad (16)$$

where $w(\tau) = \lambda_{\text{ref}} S_{\text{ref}}(\tau) + \lambda_{\text{eff}} S_{\text{eff}}(\tau) + \lambda_{\text{rare}} S_{\text{rare}}(\tau)$. This can be viewed as tilted importance sampling with target distribution $p^*(\tau) \propto p_{\text{expert}}(\tau)$, where p_{expert} is a hypothetical robust expert policy. The KL divergence between the learned policy and the expert is:

$$D_{\text{KL}}(\pi_{\theta} \| p_{\text{expert}}) = \mathbb{E}_{\tau \sim p_{\text{expert}}}[\log p_{\text{expert}}(\tau) - \log \pi_{\theta}(\tau)] \quad (17)$$

By aligning $\hat{p}_{\text{TopoCurate}}$ with p_{expert} , TopoCurate directly minimizes this divergence, ensuring the policy internalizes robust, efficient, and diverse strategies.

Sample Complexity Analysis. Standard outcome filtering requires $O(\epsilon^{-2})$ samples to achieve ϵ -optimal performance under uniform quality assumptions. However, when trajectory quality is heterogeneous (as in real agentic tasks), unweighted sampling incurs a penalty proportional to the quality variance $\sigma_{\text{quality}}^2$:

$$N_{\text{samples}} = O\left(\frac{\sigma_{\text{quality}}^2}{\epsilon^2}\right) \quad (18)$$

TopoCurate reduces $\sigma_{\text{quality}}^2$ by filtering out low-quality trajectories, lowering the sample complexity to $O(\epsilon^{-2})$ with a smaller constant factor. Empirically, TopoCurate achieves comparable performance with 30% fewer trajectories (see Table 3).

Handling Degenerate Cases: When the trajectory pool lacks diversity (e.g., all successful paths are topologically identical), our metrics naturally degrade to uniform weighting, ensuring the method does not over-penalize limited data.

C.3 Theoretical Analysis Related to Task Selection

Problem Formulation: RL Gradient Informativeness. In sparse-reward RL with Group Relative Policy Optimization (GRPO), the policy gradient is:

$$\nabla_{\theta} J(\theta) = \mathbb{E}_{\mathcal{T} \sim P_{\text{task}}} \mathbb{E}_{\{\tau_k\}_{k=1}^K \sim \pi_{\theta}(\cdot|\mathcal{T})} \left[\sum_{k=1}^K \nabla_{\theta} \log \pi_{\theta}(\tau_k) \cdot \hat{A}(\tau_k) \right] \quad (19)$$

where $\hat{A}(\tau_k) = r(\tau_k) - \bar{r}$ is the group-relative advantage. The gradient’s Signal-to-Noise Ratio (SNR) is:

$$\text{SNR} = \frac{\|\mathbb{E}[\nabla_{\theta} J]\|^2}{\text{Var}[\nabla_{\theta} J]} \quad (20)$$

Standard task selection (e.g., uniform sampling or pass-rate thresholds) fails to account for the structural properties of tasks that determine SNR, leading to two failure modes:

Failure Mode 1: Vanishing Gradients from Homogeneous Rollouts. Consider a task $\mathcal{T}_{\text{trivial}}$ where all K rollouts yield identical outcomes (either all succeed or all fail). The advantage variance is:

$$\text{Var}[\hat{A}] = \frac{1}{K} \sum_{k=1}^K (\hat{A}(\tau_k) - 0)^2 = 0 \quad (21)$$

since $\hat{A}(\tau_k) = r - \bar{r} = 0$ for all k . Consequently, $\nabla_{\theta} J \approx 0$, providing no learning signal. The expected gradient magnitude is bounded by:

$$\|\mathbb{E}[\nabla_{\theta} J]\| \leq \|\nabla_{\theta} \log \pi\| \cdot \text{Var}[\hat{A}]^{1/2} \quad (22)$$

For tasks with $\text{Var}[\hat{A}] \approx 0$, the gradient vanishes regardless of the policy’s capacity. TopoCurate avoids such tasks by prioritizing high Error Branch Ratio (V_{struct}), ensuring $\text{Var}[\hat{A}] \gg 0$.

Failure Mode 2: Low Gradient Variance from Mode Collapse. Consider a task $\mathcal{T}_{\text{single-path}}$ solvable via only one tool sequence. All successful rollouts follow the same path, leading to low policy entropy:

$$H(\pi_{\theta}|\mathcal{T}) = - \sum_{\tau} \pi_{\theta}(\tau|\mathcal{T}) \log \pi_{\theta}(\tau|\mathcal{T}) \rightarrow 0 \quad (23)$$

Low entropy implies the policy has converged prematurely to a single mode, suppressing exploration. The Fisher information matrix $\mathcal{I}(\theta)$ quantifies the sensitivity of the policy:

$$\mathcal{I}(\theta) = \mathbb{E}_{\tau \sim \pi_{\theta}} [\nabla_{\theta} \log \pi_{\theta}(\tau) \nabla_{\theta} \log \pi_{\theta}(\tau)^{\top}] \quad (24)$$

For single-mode distributions, $\mathcal{I}(\theta)$ has low rank, limiting gradient diversity. TopoCurate selects tasks with high Strategic Heterogeneity (V_{div}), ensuring $\mathcal{I}(\theta)$ remains full-rank and gradient updates explore diverse directions.

Optimality of Structural Metrics. TopoCurate defines the task sampling distribution as:

$$P_{\text{select}}(\mathcal{T}) \propto \exp\left(\frac{V_{\text{struct}}(\mathcal{T}) + \alpha V_{\text{div}}(\mathcal{T})}{T}\right) \quad (25)$$

This prioritizes tasks where:

- High V_{struct} ensures sharp decision boundaries, maximizing $\text{Var}[\hat{A}]$ and gradient magnitude.
- High V_{div} ensures multiple valid solution paths, maximizing $\text{rank}(\mathcal{I}(\theta))$ and preventing premature convergence.

The expected SNR under TopoCurate’s distribution is:

$$\mathbb{E}_{\mathcal{T} \sim P_{\text{select}}}[\text{SNR}] \propto \mathbb{E}[V_{\text{struct}}] \cdot \mathbb{E}[V_{\text{div}}] \quad (26)$$

Maximizing this expectation directly optimizes for gradient informativeness.

Connection to Fisher Information and Natural Gradients. The Fisher information matrix $\mathcal{I}(\theta)$ defines the natural gradient:

$$\tilde{\nabla}_{\theta} J = \mathcal{I}(\theta)^{-1} \nabla_{\theta} J \quad (27)$$

Natural gradients converge faster than standard gradients by accounting for the curvature of the policy manifold. Tasks with high V_{struct} and V_{div} increase the smallest eigenvalue $\lambda_{\min}(\mathcal{I}(\theta))$, reducing the condition number $\kappa = \lambda_{\max}/\lambda_{\min}$ and accelerating convergence. Formally:

$$\|\theta^{(t+1)} - \theta^*\| \leq \left(1 - \frac{\eta}{\kappa}\right) \|\theta^{(t)} - \theta^*\| \quad (28)$$

where θ^* is the optimal policy. By improving κ , TopoCurate accelerates RL training.

Sample Efficiency Bounds. For standard task selection with uniform sampling, the sample complexity to achieve ϵ -optimal policy is:

$$N_{\text{tasks}} = O\left(\frac{|\mathcal{A}|^2 |\mathcal{S}|^2}{\epsilon^2 (1 - \gamma)^4}\right) \quad (29)$$

where $|\mathcal{A}|, |\mathcal{S}|$ are the action and state space sizes, and γ is the discount factor. TopoCurate reduces this by a factor proportional to the average SNR:

$$N_{\text{tasks}}^{\text{TopoCurate}} = O\left(\frac{|\mathcal{A}|^2 |\mathcal{S}|^2}{\epsilon^2 (1 - \gamma)^4 \cdot \mathbb{E}[\text{SNR}]}\right) \quad (30)$$

Robustness to Task Distribution Shift. In deployment, the test task distribution $p_{\text{test}}(\mathcal{T})$ may differ from training. Tasks with high structural diversity (high V_{div}) provide better generalization. Formally, the generalization gap is bounded by:

$$\mathbb{E}_{\mathcal{T} \sim p_{\text{test}}}[J(\theta)] - \mathbb{E}_{\mathcal{T} \sim p_{\text{train}}}[J(\theta)] \leq C \cdot D_{\text{KL}}(p_{\text{test}} \| p_{\text{train}}) \quad (31)$$

TopoCurate minimizes this gap by training on structurally diverse tasks, reducing the effective D_{KL} through improved coverage of the task manifold.

Robustness in Low Data Regimes: In scenarios where trajectory data is sparse, the topological structure may be underdeveloped. In such cases, TopoCurate naturally degrades to a uniform sampling strategy (as $\Phi(v)$ becomes uniform), providing a *safe fallback mechanism*.

D Case Studies From TAU2

D.1 Trajectory Comparison for Agent Behaviours

At the trajectory level, we compare multiple successful trajectories within the same task. Regarding diversity, different correct trajectories for the same task exhibit distinct step-by-step procedures and reasoning paths, such as what information is checked first, how the problem is decomposed, and how the agent transitions between subtasks.

Trajectory Comparison — Diversity

Task:	Change the existing flight/reservation from JFK to LAX to a flight to the Bay Area (SFO or OAK), and strongly prefers not to cancel and rebook.
Trajectory 1:	Treat the issue as a "rules/system boundaries" problem. First, clearly explain whether the destination can be changed, and then move on to the next steps.
Typical steps:	Collect identity and order information → Confirm facts/background → Clarify hard constraints → Provide actionable solutions within the constraints
Trajectory 2:	Quickly reject infeasible requests, then immediately provide the information needed for the user's decision (flights/prices).
Typical steps:	Collect identity and order information → Provide a quick conclusion → Immediately present alternative solutions → Give guidance for the next step
Comparison:	Trajectory 1: First, explain the rules thoroughly, then proceed. Trajectory 2: Directly give the conclusion, then provide the alternative flight prices.

Regarding efficiency, we contrast pairs of trajectories that share the same starting conditions and reach the same successful outcome. Despite achieving identical results, they differ in their intermediate steps and overall length, reflecting distinct ways of organizing the process like using a single consolidated processing loop versus a phased multi-turn progression.

Trajectory Comparison — Efficiency

Task:	The user needs to modify the pending order, changing the T-shirt size from M to L and the shoe color from black to blue. Confirm the price difference and use the \$75 gift card balance to cover any extra cost.
Current State:	The user wants to modify the pending order and has completed email verification. The next step is to locate the order and process the changes and price difference payment.
Trajectory 1:	After email verification, merge the process for a single cycle, shorter.
Typical steps:	Email verification → Locate pending order → Check product variants / calculate price difference → Confirm gift card balance can cover → User confirmation → Submit modification and return success result
Trajectory 2:	After email verification, proceed in phases, with additional calculation steps, resulting in multiple cycles, longer.
Typical steps:	Email verification → Output order status / summary and confirm pending → User clarifies modification request → Check product variants + additional price difference calculation → Confirm gift card availability → User confirmation → Submit modification and return success result
Comparison:	With the same user introduction and goal, Trajectory 1: Combine processing (locating the order and addressing modification requests in one step), making it shorter. Trajectory 2: Use "phased processing (first confirming the order, then having the user restate their request) + additional calculation steps," making it longer.

D.2 Task Comparison for Training Potential Evaluation

At the task level, we observe that even when two tasks have a similar number of correct trajectories or comparable success rates, they may still show significant differences in the number of valid Solution Families they contain. This reveals the varying degrees of convergence or diversity manifested in the overall structure of the tasks.

Task Comparison

Task 1:	The user is unable to send MMS (multimedia messages) and needs to troubleshoot and restore functionality.
Solution type:	Type 1: Connectivity → permissions closure: restore connectivity first (enable mobile data, reset SIM, etc.), then identify missing SMS permission and enable it to fix MMS. Type 2: SIM-first → permissions convergence: fix SIM/no-signal issues first, then enable missing SMS permission to resolve MMS.
Task 2:	The user is in France and experiencing slow or intermittent mobile data, requesting "excellent speed."
Solution type:	Type 1: Usage/limit-first + settings optimization: refuel/add data first, then enable data roaming and disable Data Saver, reaching "excellent" speed in a speed test. Type 2: Settings-first (roaming → data saver): enable Data Roaming first, then disable Data Saver to improve speed. Type 3: Settings-first (data saver → roaming): disable Data Saver first, then enable Data Roaming. Type 4: Recovery/backtracking type: after a setting change causes loss of connectivity or user anxiety, proceed with step-by-step checks/restart, and still end up with the combo fix.
Comparison:	Task 1: 8 correct trajectories, 2 types, more "convergent" (most correct trajectories fall into a few ending shapes). Task 2: 8 correct trajectories, 4 types, ending shapes are more dispersed (more types).